Supporting Information for

Purcell Enhanced Photoluminescence of Few-layer MoS_2 Transferred on Gold Nanostructure Array with Plasmonic Resonance at Conduction Band Edge

Hyunwoo Kim,[§,‡] *Seunghyun Moon,* [‖,‡] *Jongwoo Kim,*[@] *Sang Hwan Nam,*[§] *Dongwan Kim,*[‖] *Jeong Seop Lee,*[¶] *Kyoung-Ho Kim,*[¶] *Evan S. H. Kang,*[¶] *Kwang Jun Ahn, Taewan Kim*[©,*], *Chaeho Shin,*[‖,*] *Yung Doug Suh,*[§,#,*]

[§] Interdisciplinary Materials Measurement Institute, Korea Research Institute of Standards and Science, Daejeon 34113, South Korea

[‖] Interdisciplinary Materials Measurement Institute, Korea Research Institute of Standards and Science, Daejeon 34113, South Korea

[@] Center for Convergent Research of Emerging Virus Infection, Korea Research Institute of Chemical Technology, Daejeon 34114, South Korea

¶ Department of Physics, Chungbuk National University, Cheongju, Chungbuk 28644, South Korea

© Department of Electrical Engineering and Smart Grid Research Center, Jeonbuk National University, Jeonju, 54896, South Korea

School of Chemical Engineering, Sungkyunkwan University, Suwon 16419, South Korea

KEYWORDS : Purcell effect, localized surface plasmon, molybdenum disulfide, plasmonic enhancement

1. AFM measurement for thickness characterization of few-layer MoS_2 film

For the characterization of layer thickness of MoS_2 film transferred on the Au nanoparticle array substrate, AFM morphology of the substrate was obtained. AFM was operated in a non-contact mode equipped with NCHR probe (NanoSensors). The cross section profile of the AFM morphology (Figure S1, bottom) shows the MoS2 film height of ~4.7 nm. The number of MoS2 layer is estimated to be ~7 based on the interlayer distance of MoS_2.[1]

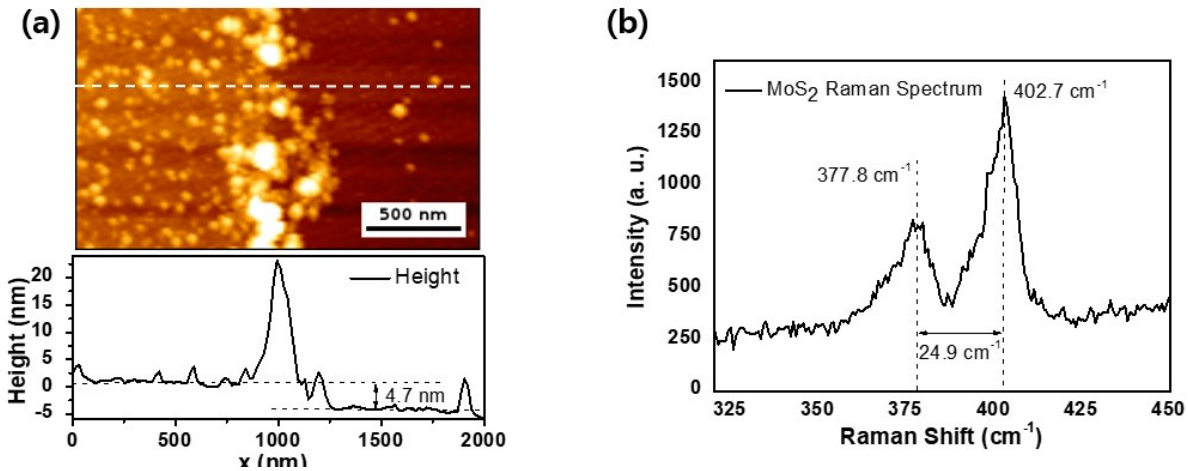

Figure S1. (a) AFM thickness measurement of few-layer MoS_2 film transferred onto the substrate with Au nanoparticle array. (Top) AFM morphology of few-layer MoS_2. The scale bar is 500 nm. (Botton) Cross-section profile of the AFM morphology along the x-axis. (b) Raman scattering spectra of MoS_2 layer measured with excitation wavelength of 532 nm.

2. Full wave optical simulation calculated optical near-field amplitude of Au nanotriangle

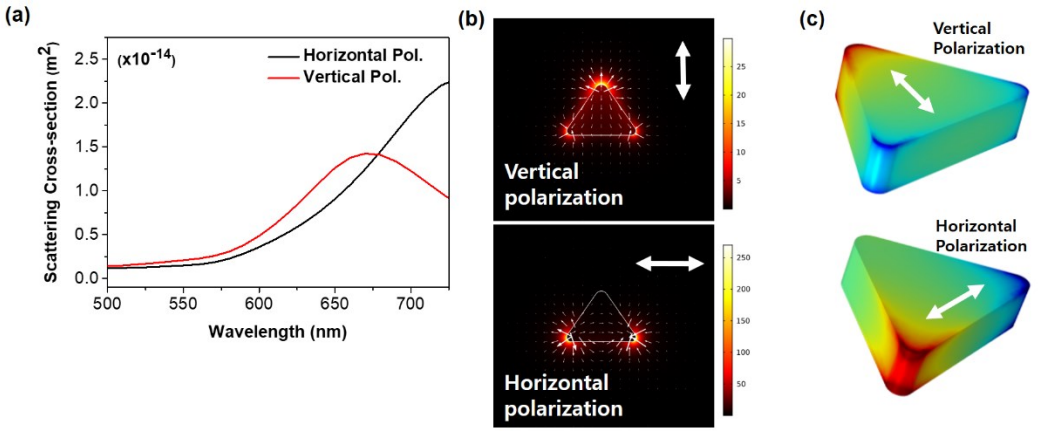

Figure S2. (a) Full-wave optical simulation calculated scattering optical cross section of Au nanotriangle (NT) with baseline length of 120 nm and equilateral lengths of 90 nm. (b) Field intensity profile of Au NT with vertical (top) and horizontal (bottom) incident polarization. (c) Surface charge density of Au NT excited by vertical (top) and horizontal (bottom) incident polarization.

3. PL enhancement factor of single plasmonic nanostructure with diffraction-limited focus area correction

In the measurement of plasmonic enhanced PL, there is significant mismatch between the focus area of irradiation and the cross-section of plasmonic nanostructures. Because the area of plasmonic nanostructures with LSPR are usually much smaller than the diffraction-limited focus area of the incident light, PL enhancement factor (EF) obtained from PL intensities of nanostructure combined MoS_2 film often underestimate PL EF induced by single nanostructure. For the precise estimation of single plasmonic nanostructure contribution to PL

enhancement of MoS_2, correction factor needs to be applied to experimentally measured PL spectra which takes area mismatch between focal spot and the nanostructures into consideration. In this section, we describe the derivation of the area correction factor based on geometrical interpretation of PL emission intensities.

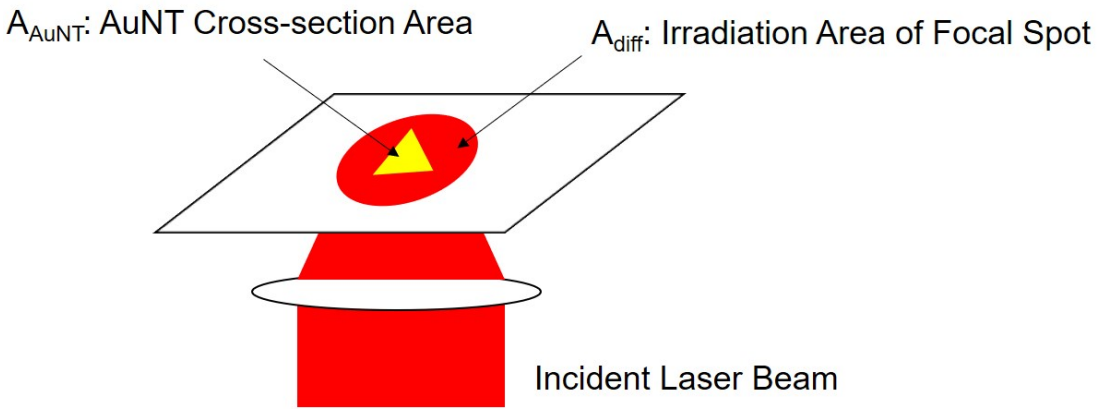

Figure S3. Schematic of optical excitation of plasmonic nanostructure (Au NT) combined with MoS_2 layer. Incident laser beam is focused into the focal spot area (A_{diff}) for irradiation and plasmonic optical concentration takes place in the close proximity to Au NT within the cross section area (A_{AuNT}).

The PL intensities of MoS_2 excited by focused incident light on bare MoS_2 layer (I_{diff}) are assumed to be proportional to the irradiation area, which can be described by

$$I_{diff} = A_{diff} \cdot \varepsilon_{bare} \qquad \text{(Eq. S1)}$$

, where A_{diff} is focal spot area, and ε_{bare} is PL emission efficiency of bare MoS_2 layer per unit irradiation area. The PL intensities of MoS_2 combined with nanostructures can be modelled as follow,

$$I_{AuNT} = A_{AuNT} \cdot \varepsilon_{AuNT} + (A_{diff} - A_{AuNT}) \cdot \varepsilon_{bare} \qquad \text{(Eq. S2)}$$

, where A_{AuNT} is cross-section area of plasmonic nanostructure, and ε_{AuNT} is PL emission

efficiency of MoS_2 layer combined with nanostructure per unit irradiation area. The PL EF is given by the PL intensity of MoS_2 combined with nanostructure, which is divided by that of bare MoS_2 without nanostructure, as following

$$EF = \frac{I_{AuNT}}{I_{diff}} \approx 1 + \frac{A_{AuNT}\varepsilon_{AuNT}}{A_{diff}\ \varepsilon_{bare}} \quad \text{(Eq. S3)}$$

The PL EF induced by single nanostructure without any irradiation area dependency can be derived from Eq. S3 as following

$$EF_{AuNT} = \frac{\varepsilon_{AuNT}}{\varepsilon_{bare}} = (\frac{I_{AuNT}}{I_{diff}} - 1) \cdot \frac{A_{diff}}{A_{AuNT}} \quad \text{(Eq.S4)}$$

, where A_{diff}/A_{AuNT} is defined as the focus area correction factor. In brief, PL enhancement factor of single nanostructure can be estimated by multiplying the focus area correction factor to the PL enhancement ratio normalized by PL intensity of bare MoS_2.

The focus area correction factor can be calculated by using experimental parameters such as numerical aperture of focusing lens, and excitation wavelength.

The diffraction-limited focus area can be given by,

$$A_{diff} = \pi(\frac{\lambda}{2NA}/2)^2 \quad \text{(Eq. S5)}$$

, where λ is the wavelength of the incident light, and NA is the numerical aperture of focusing lens. The cross section area of plasmonic nanostructure can be obtained from SEM images.

4. SEM and optical scattering spectra of Au nanodisk

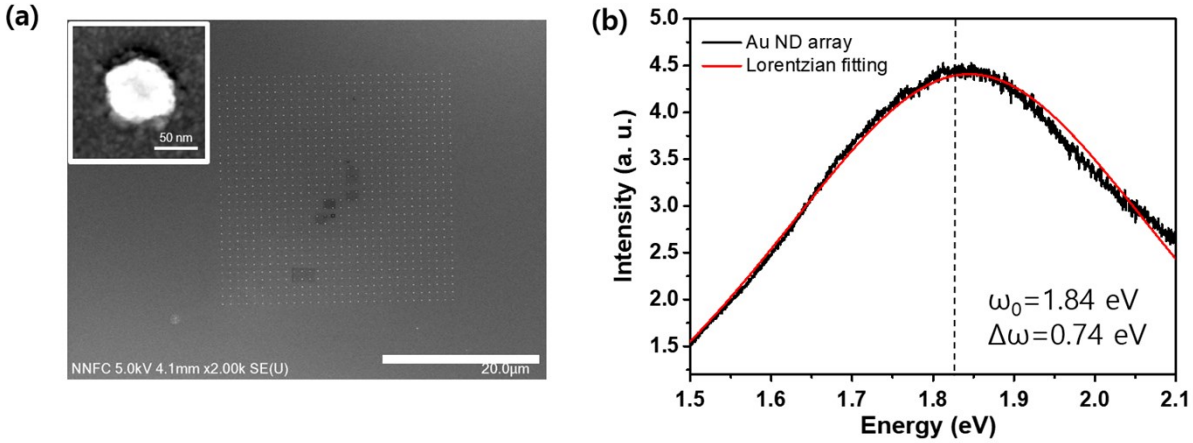

Figure S4. (a) SEM image of Au nanodisk (ND) array. Scale bar is 20 μm. Magnified image of single Au ND. Scale bar is 50 nm. (b) Optical scattering spectrum of Au ND normalized by background spectrum measured from blank area without Au ND (black line). The spectrum is fitted with Lorentzian curve which is centered at 1.84 eV (~670 nm) with peak width of 0.74 eV, resulting in Q-factor of 2.49.

5. SEM and optical scattering spectra of Au nanodisk

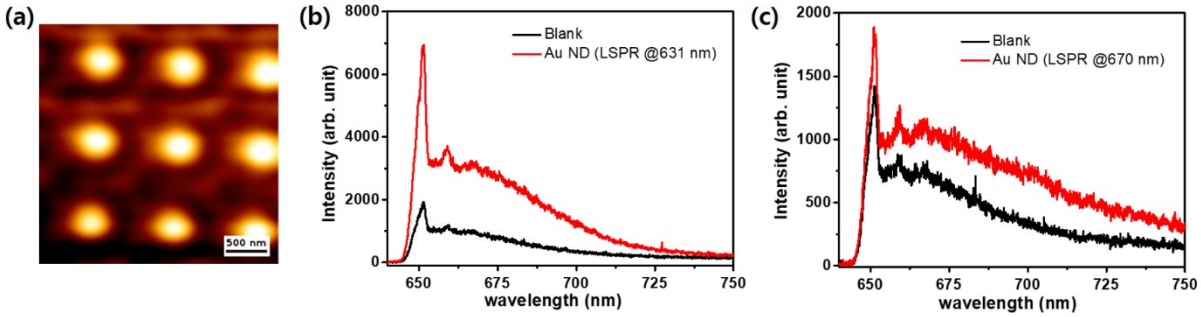

Figure S5. (a) Stage raster scanned confocal image of AuND array with the focal spot position of 633 nm incident laser is fixed. The reflected and Rayleigh scattering signal were recorded by APD without longpass filter. (b, c) Photoluminescence spectra measured from bare MoS_2 layer (black line), and from MoS_2 layer combined with single Au ND (red line), which have LSPR resonance at 631 nm (b), and 670 nm (c), respectively.

6. Purcell enhancement factor correction due to the spectral mismatch between the resonances of nanoresonator (LSPR) and emitter (excited carriers of MoS_2)

Spectral mismatch between the resonances of Au NT LSPR (ω_0) and the direct bandgap of MoS_2 (ω) cause reduction of Purcell factor. The reduction of the decay rate Γ of the excited carriers assuming Lorentzian line shapes for PL emission and LSPR mode can be considered as following,[2]

$$\Gamma / \Gamma_0 = F \frac{\omega_0^2}{\omega^2} \frac{\omega_0^2}{\omega_0^2 + 4Q^2(\omega - \omega_0)^2} \qquad \text{(Eq. S6)}$$

,where Γ_0 is the decay rate of excited carriers in bare MoS_2 layer without coupling with Au NT. Taking the Q-factor of Au NT array of ~5.5, ω_0 centered at 667 nm, and ω centered at 660 nm into consideration, reduction of Purcell factor due to the spectral detuning between direct bandgap energy of MoS_2 and LSPR mode was estimated to be ~4.2%.

7. Optical setup schematic for stage raster scanning PL measurement

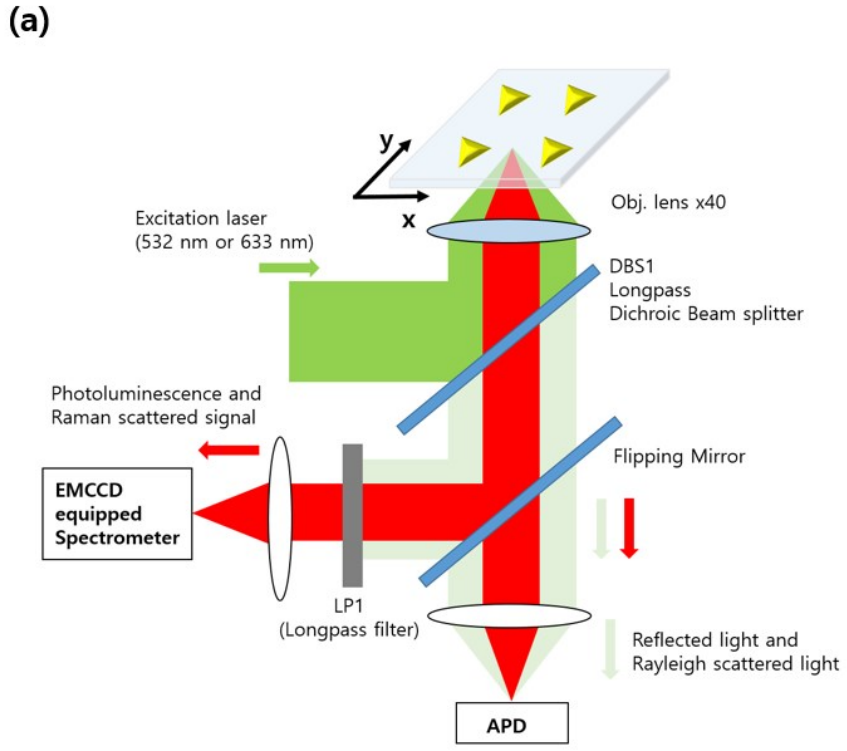

Figure S6. Stage raster scanning photoluminescence (PL) measurement of MoS_2 layer transferred on nanostructure array. Excitation laser sources (532 nm and 633 nm) are focused onto the substrate by objective lens (NA=0.6) through epi-illumination geometry. PL from MoS2 layer and scattering from nanostructures are collected by the same objective lens. Cutoff wavelength of longpass dichroic beamsplitter (DBS1) and longpass filter (LP1) were changed in accordance with the excitation wavelength. Flipping mirror was flipped-on to direct the signal beam toward EMCCD equipped with spectrometer for PL spectrum measurement, while the mirror is flipped-off to pass the signal beam toward APD for the Rayleigh scattering signal measurement.

1. Mak, K. F.; Lee, C.; Hone, J.; Shan, J.; Heinz, T. F. *Physical Review Letters* **2010,** 105, (13), 136805.
2. Sauvan, C.; Hugonin, J. P.; Maksymov, I. S.; Lalanne, P. *Physical Review Letters* **2013,** 110, (23), 237401.